Eur. Phys. J. A **31**, 868–874 (2007)
DOI 10.1140/epja/i2006-10240-4

THE EUROPEAN PHYSICAL JOURNAL A

Special Article – QNP 2006

Latest results on the hot dense partonic matter at RHIC

M.J. Leitch[a]

Los Alamos National Laboratory, Los Alamos, NM 87545, USA

Received: 8 November 2006
Published online: 9 March 2007 –

Abstract. At the Relativistic Heavy-Ion Collider (RHIC) collisions of heavy ions at nucleon-nucleon energies of 200 GeV appear to have created a new form of matter thought to be a deconfined state of the partons that ordinarily are bound in nucleons. We discuss the evidence that a thermalized partonic medium, usually called a Quark Gluon Plasma (QGP), has been produced. Then, we discuss the effect of this high-density medium on the production of jets and their pair correlations. Next, we look at direct photons as a clean electro-magnetic probe to constrain the initial hard scatterings. Finally, we review the developing picture for the effect of this medium on the production of open heavy quarks and on the screening by the QGP of heavy-quark bound states.

PACS. 25.75.-q Relativistic heavy-ion collisions – 24.85.+p Quarks, gluons, and QCD in nuclei and nuclear processes

1 Introduction

The collisions of high-energy heavy ions are thought to form very high temperatures and densities similar to those that occurred in the earliest stages of our Universe. These collisions are thought to create matter with energy densities up to 30 times normal nuclear-matter density in a small region ($\sim 10^{-14}$ m) and for a short time ($\sim 10^{-23}$ s). Different experimental probes examine different stages of the matter as it expands and evolves back to normal matter. Hard probes created in the initial collisions before thermalization of the medium probe the medium through their final-state interactions. Soft probes come from the medium itself and provide a picture of its thermalization and spatial evolution.

Here we will review the most significant results from the RHIC heavy-ion program and discuss their implications in terms of the nature of the hot-dense matter that is created in these collisions. I thank many colleagues at RHIC for helping me prepare this review, especially Akiba, Constantin, d'Enterria, Granier de Cassagnac, Jacak, Nagle, Seto, and Zajc.

2 RHIC and its detectors

The Relativistic Heavy-Ion Collider (RHIC) collides Au ions at center-of-mass energies per nucleon pair of up to 200 GeV, substantially higher in energy than the 17 GeV at the CERN SPS, but lower than the 5.5 TeV anticipated at the LHC. At RHIC four experiments, two large (PHENIX and STAR) and two small (BRAHMS and PHOBOS) experiments observe the collisions and together have advanced our understanding considerably since the first collisions at RHIC. Each experiment has different strengths with BRAHMS having two classic dipole spectrometers, PHOBOS focusing on extensive silicon-strip detectors, PHENIX being a complex many-subsystem detector optimized for rare probes, and STAR centered around a large solid-angle TPC.

In heavy-ion collisions, an important aspect one studies for all observables is their dependence on the centrality of the collision, *i.e.* whether a particular collision is "head-on" (central or, *e.g.*, 0–10% centrality) or peripheral (*e.g.*, 80–90%) with only the edges of the two colliding nuclei passing through each other. An approximate centrality measurement for each collision is obtained with a combination of the measured charged-particle multiplicity and the yield of spectator neutrons that are observed in zero-degree calorimeters (ZDC). These measurements are related to the actual centrality using a simple Glauber model of the collision.

3 Thermalization

One of the key issues in high-energy heavy-ion collisions is the time scale and the degree to which the available energy is thermalized into a medium. Several of the soft-sector observables give us important information on this aspect of the collisions.

[a] e-mail: leitch@bnl.gov

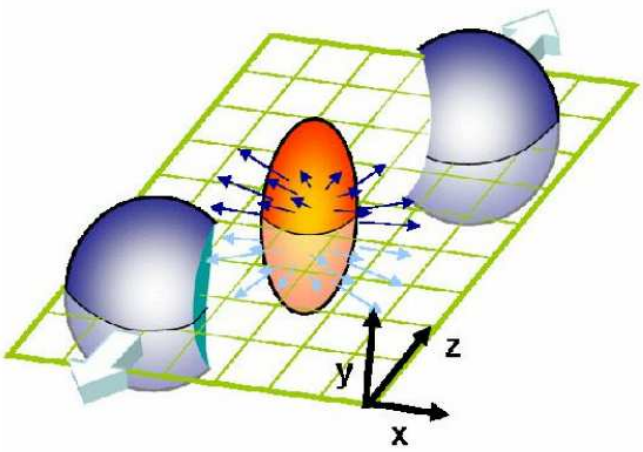

Fig. 1. Cartoon showing the initial geometrical asymmetry in a non-central heavy-ion collision.

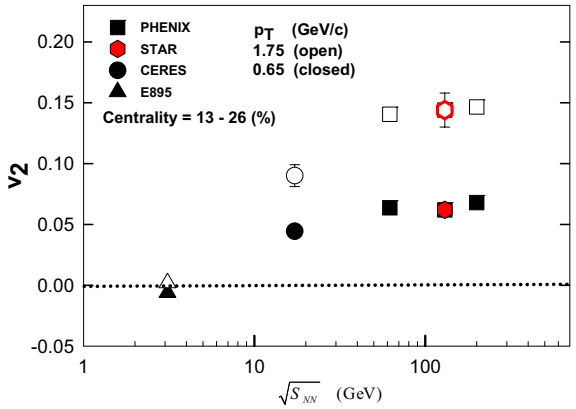

Fig. 2. Dependence of the flow or v_2 of hadrons on center-of-mass energy, $\sqrt{s_{NN}}$, for two different transverse momentum (p_T) values [1].

The first is the extent to which the observed lower-momentum produced particles exhibit "hydrodynamic flow" as would be expected from a thermalized medium. For not fully head-on collisions, as shown in fig. 1, an asymmetric or almond-shaped collision region is produced. This initial anisotropy is converted into a corresponding momentum anisotropy which results in an azimuthal asymmetry relative to the reaction plane in the yield of produced particles at a given momentum. The efficiency of this conversion depends on the properties of the medium, with large asymmetries corresponding to early thermalization. This asymmetry is usually represented by "v_2" which is the 2nd Fourier coefficient of the momentum anisotropy,

$$\mathrm{d}n/\mathrm{d}\phi \sim 1 + 2v_2(p_T)\cos(2\phi) + \ldots . \qquad (1)$$

The observed flow tends to saturate near RHIC energies [1], as shown in fig. 2, suggesting that early thermalization has been achieved. Also supporting early thermalization are comparisons with hydrodynamics calculations which indicate that the flow observed at RHIC is near the maximal flow predicted by the models. However, ongoing

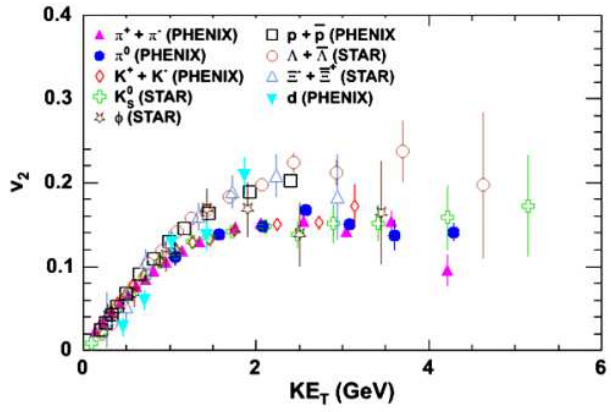

Fig. 3. Flow for hadrons *vs.* transverse energy, $KE_T = m_T -$ mass.

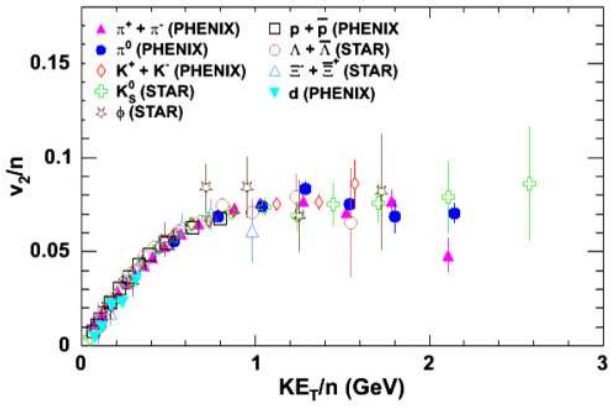

Fig. 4. Flow per quark *vs.* transverse energy per quark, KE_T/n.

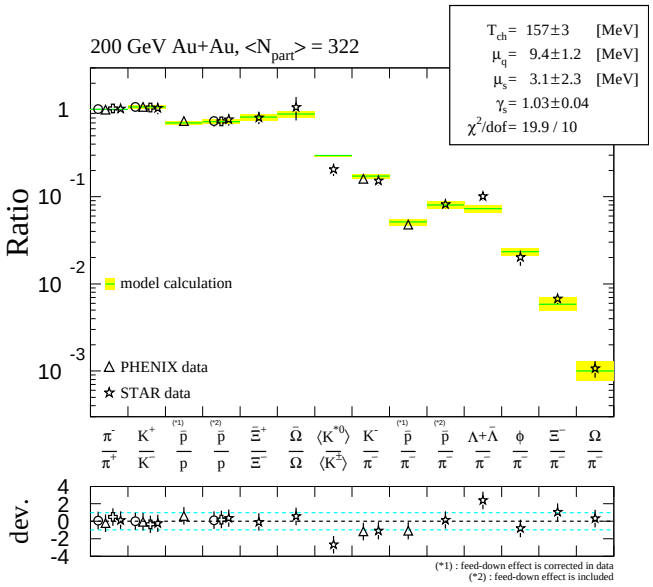

Fig. 5. Ratios of hadron yields are well reproduced by statistical combination models based on quark degrees of freedom.

improvements in the hydrodynamic models may shed new light on what the true limits are.

Another important aspect of the flow measurements is that when comparisons of the flow for different particles are made there are substantial differences observed, see fig. 3. However, if one plots the flow normalized to the number of valence quarks in the observed hadron *vs.* the transverse kinetic energy per quark, fig. 4, a universal behavior emerges. This supports a picture where the relevant degrees of freedom of the thermalized medium are quarks, *i.e.* the thermalization occurs when the matter is not hadrons but consists of deconfined quarks.

Finally, statistical models that reproduce ratios of hadron yields [2], such as those in fig. 5, also support a picture where the degrees of freedom are quarks up to the "freezeout" time when the observed hadrons form.

4 Jets and energy loss

Arguably, the most dramatic effect seen at RHIC so far, is the strong suppression of high-p_T hadrons in the most central Au + Au collisions compared to p + p collisions. Although it has not been possible in the high-multiplicity environment of Au + Au collisions at RHIC to fully reconstruct jets, these high-p_T particles should be good surrogates for the jets. As shown in fig. 6, π^0's are suppressed by more than a factor of two in central Au + Au collisions, but have little or no modification for the cold–nuclear-matter control measurement in d + Au collisions. This is interpreted as evidence for large energy losses of the jets in the final state where they traverse the hot high-density matter created in the Au + Au collisions. Models infer from this that matter densities of ~ 15 times normal nuclear-matter density are involved in the earliest stages, before expansion, of the created medium.

In addition to studying the yield of hadrons *vs.* p_T, the correlation of hadron pairs has also been studied. In this case a "tag" is provided by one high-p_T hadron, and then the distribution of other hadrons in the same event

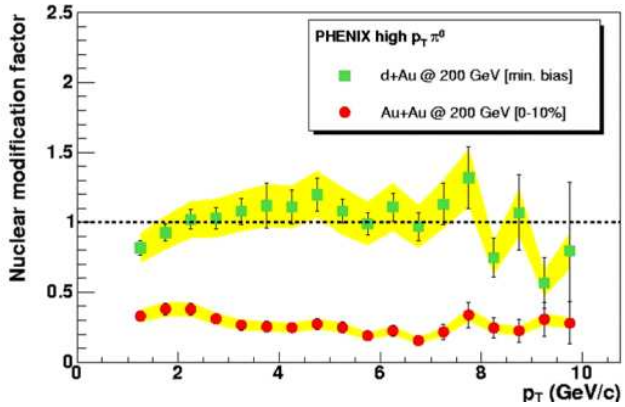

Fig. 6. (Colour on-line) Large suppression of the π^0 yield per binary collision in Au + Au collisions (red circles) contrasted with lack of suppression for d + Au collisions (green squares) [3].

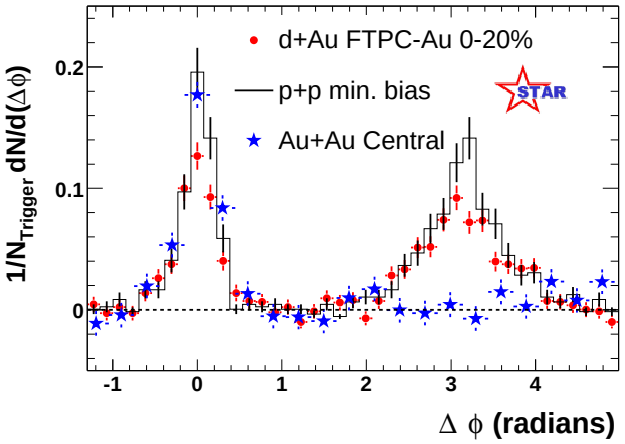

Fig. 7. (Colour on-line) Distribution in azimuthal angle (ϕ), with respect to a tagging high-p_T ($p_T = 4$–$6\,\mathrm{GeV}/c$) particle, of other particles ($p_T > 2\,\mathrm{GeV}/c$) seen in the same event for central Au + Au collisions (blue stars), compared to d + Au collisions (red dots) and p + p collisions (black histogram and vertical bars) [4].

is observed. Figure 7 shows these correlations for central Au + Au, central d + Au and p + p collisions. In d + Au collisions the correlation is essentially unaltered from that for p + p collisions, while for central Au + Au collisions the "away-side" correlation ($\Delta\phi \sim \pi$) disappears, with the "near-side" peak (other particles associated with the jet that the tagging particle is from) remains like that of p + p and d + Au. This result is usually interpreted as a tagging jet coming from near the surface and a partner "away-side" jet that is degraded by the thick high-density medium it has to pass through on the other side. Further studies looking at lower momenta for the "away-side" hadrons appear to find remnants of this jet in broad distributions of low-momentum particles. In some momentum windows these "away-side" particles even show a very interesting split distribution with a depression in their yield for exactly back-to-back angles, and side maxima. This phenomena has been interpreted by some as evidence for "mach-cone" effects in the medium [5].

5 Direct photons and the initial state

Direct photons, although difficult to isolate experimentally, because of their weak electromagnetic interaction with the medium in the final state, connect directly to the initial state where the hard interactions take place —before the thermalization of the medium. In fig. 8 the direct photons in central Au + Au collisions show that the initial state is not modified from that of p + p collisions, while the neutral mesons (as discussed above) are strongly suppressed due to final-state effects in the hot dense medium. This comparison affirms the idea discussed above, that the observed hadron jet modifications do come from the final state.

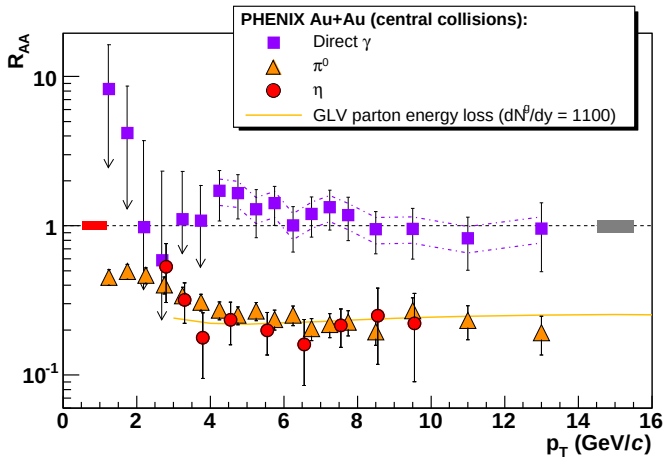

Fig. 8. (Colour on-line) Direct photons (purple squares) are not suppressed in central Au + Au collisions as compared to the strong suppression seen for π^0's (yellow triangles) and η's (red circles) [6]. The solid curve is a parton energy loss calculation [7].

6 Heavy quarks

So far we have discussed light hadrons, including the large energy loss observed in the final state when they pass through the high-density matter created in central Au + Au collisions. Heavy quarks are expected to suffer different effects in this medium, but they are more difficult to measure both because of their smaller production cross-sections and due to the difficulty of separating them from backgrounds. Despite these difficulties, initial measurements primarily through measurements of leptons from the semi-leptonic decay of the heavy (charm and beauty) mesons are now available. In fig. 9 the suppression of non-photonic electrons at mid-rapidity from charm and beauty decays is shown. The large suppression seen, like that for light hadrons, is interpreted as energy loss in the high-density medium created in these central Au + Au collisions. Similar measurements at forward rapidity are being worked on using decays to muons, but so far results are only available for d + Au and p + p collisions. The latter are shown in fig. 10 where one sees that d + Au heavy-quark yields are suppressed at forward rapidity (small-x or shadowing region in the Au nucleus) and enhanced at backward rapidity (larger-x or anti-shadowing region). The suppression in the forward or small-x region is usually attributed to nuclear shadowing of the gluon distributions [11] or to gluon saturation models [12]; but could also involve other cold nuclear matter effects such as initial-state gluon energy loss.

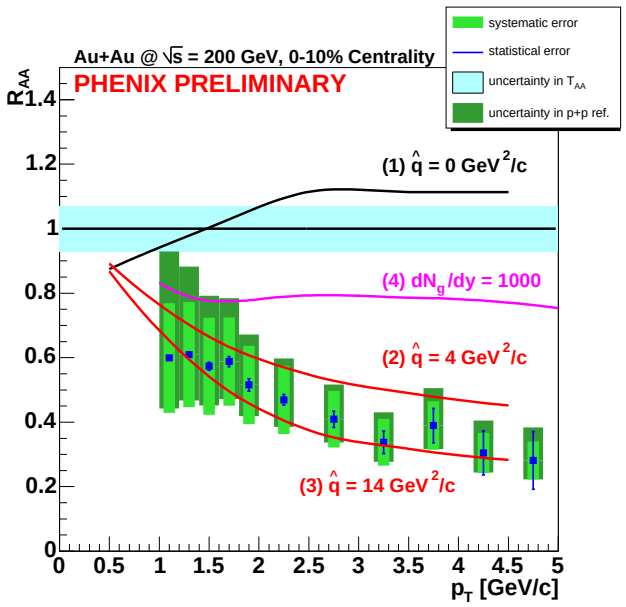

Fig. 9. Nuclear modification factor, R_{AA}, for heavy quarks at central rapidity observed using non-photonic electrons in central Au + Au collisions at 200 GeV [8].

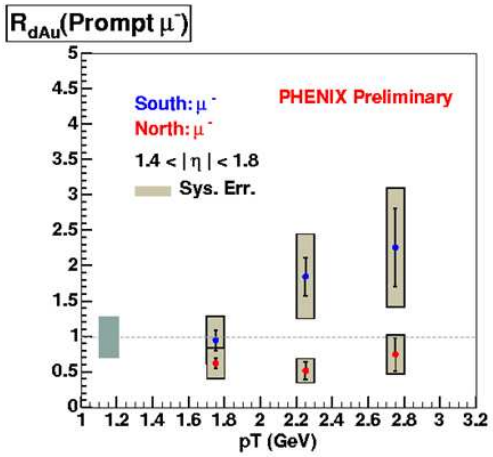

Fig. 10. Nuclear suppression factor, R_{dAu}, at forward and backward rapidity for heavy quarks observed using prompt muons (heavy quarks) in d + Au collisions at 200 GeV [9].

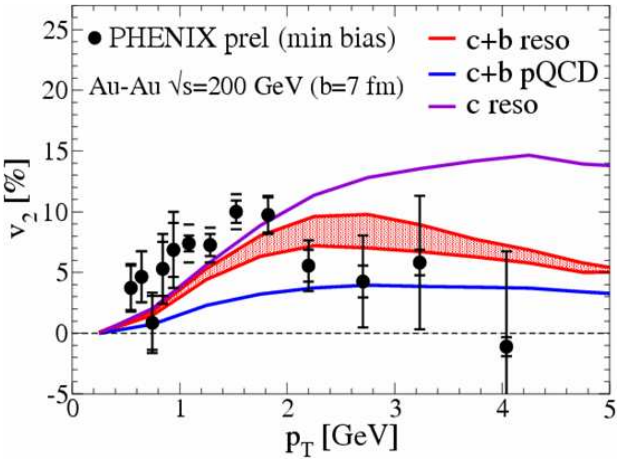

Fig. 11. (Colour on-line) Flow of heavy quarks at mid-rapidity for 200 GeV minimum-bias Au + Au collisions, as obtained from non-photonic electrons [8]. Data is compared to theoretical calculations [10] that have no flow (blue curve), only charm flow (purple curve), or both charm and beauty flow (red curve).

The electrons from heavy-quark decays have also been analyzed in terms of their elliptic flow, analogous to what was discussed above for hadrons. Surprisingly, at least for small p_T values, these heavy quarks also seem to exhibit flow (non-zero v_2), as shown in fig. 11. Although the data uncertainties remain large due to the low rates of heavy-quark production and the large systematics background subtraction, the usual interpretation of these results is that for the lowest transverse momentum the charm quarks do flow with the light quarks, but as the momentum goes up they punch through the thermalized medium and the flow disappears. However, more accurate measurements will be needed to firm up the true characteristics of heavy-quark flow (sect. 8).

7 J/ψ's and color screening in the medium

The J/ψ and other heavy quarkonia are thought to provide a key signature for a deconfined medium. Early predictions were that the two heavy quarks that would form the bound state would be screened from each other in the high-density deconfined medium [13]. This effect would depend on the size or binding energy of the specific state and so different states (J/Ψ, ψ', χ_C, Υ_{1S}, Υ_{2S}, Υ_{3S}) would "melt" at different energy densities. However, more recently, lattice QCD calculations have suggested that, in fact, the J/ψ would not be screened unless effective densities of the hot plasma created in these heavy-ion collisions exceeded twice the critical temperature [14].

The J/ψ suppression at RHIC was predicted to be larger than that observed at the SPS by most of the theoretical models that were successful in describing the SPS data [15,16]. This reflects the expectation that the matter created at RHIC would be hotter and longer-lived than that for the lower-energy SPS measurements. Contrary to this expectation, the measurements at RHIC show suppression very similar to that at lower energy. In fig. 12 are shown preliminary J/ψ measurements for Au + Au collisions from PHENIX [17], along with earlier measurements of the cold–nuclear-matter effects as seen in d + Au collisions [18] at the same energy. First, one can see that simple models that describe the poor statistics d + Au measurements for a range of absorption cross-sections give a large uncertainty in the expected cold–nuclear-matter effects for Au + Au collisions (blue on-line bands). Clearly, better d + Au data is needed to more accurately constrain the cold–nuclear-matter effects and to allow a more quantitative understanding of how much of the Au + Au suppression does not come from these effects, and how much may come from additional effects of the hot dense matter. Nevertheless, for the most central collisions, the Au + Au data clearly show a stronger suppression than one would expect from cold–nuclear-matter effects alone.

At present, we are left with two theoretical pictures which both provide a plausible explanation of the level of suppression seen in the RHIC data. One of these, shown in fig. 13, was actually a prediction from before the experimental results were obtained [16]. This model includes

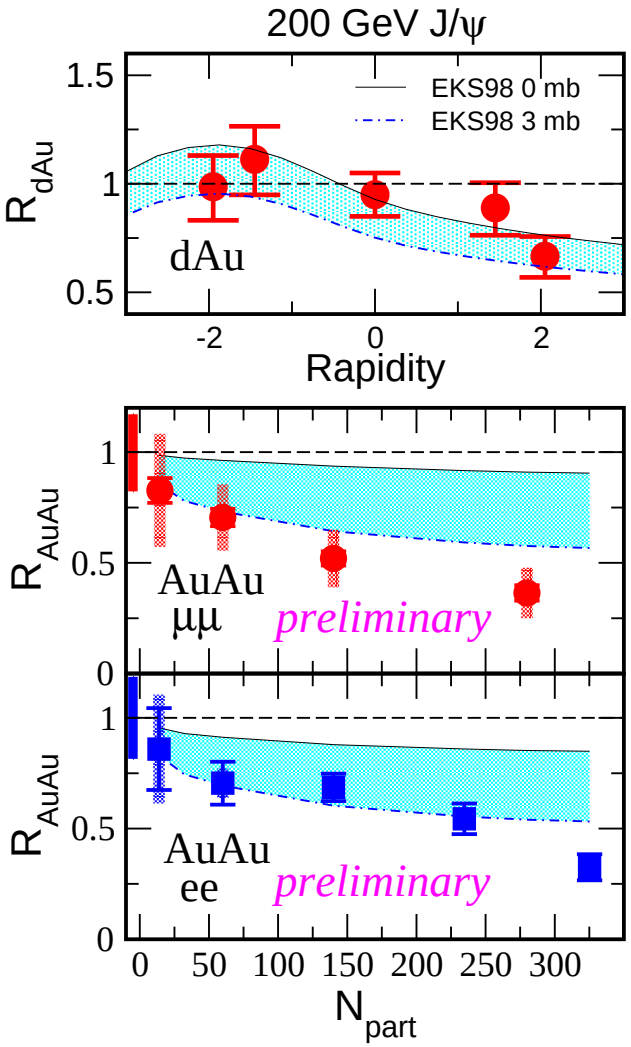

Fig. 12. (Colour on-line) Cold–nuclear-matter effects on J/Ψ production are constrained by the limited accuracy of our present d + Au data [18] (blue band in top panel). Corresponding calculations for Au + Au collisions give bands on the bottom panels for forward rapidity (middle panel) and central rapidity (bottom panel) data [17]. N_{part} is the number of participants, and is a measure of the centrality of the Au + Au collision.

strong dissociation of the charm pairs from the large gluon density created in the collisions (analogous to screening), but also includes regeneration of bound charm pairs (J/ψ's) in the later stages of the expansion driven by the large production and high density of independently produced charm quarks. So in this model, there is a stronger "screening" effect at RHIC than at the SPS but it is compensated for by the regeneration, resulting in a net suppression very similar to that seen at the SPS.

The second picture, sequential screening [19], asserts that (as suggested by recent lattice calculations) the J/ψ is not screened in central Au + Au collisions at RHIC or at SPS energies. Rather the observed suppression comes only from screening of the higher-mass states, χ_C and ψ',

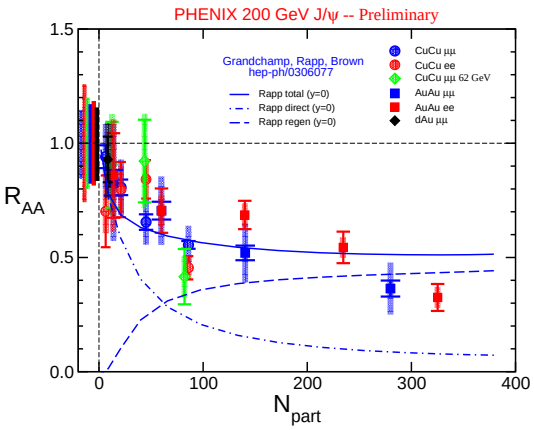

Fig. 13. Comparison *vs.* centrality of the Au + Au J/ψ data [17] to theoretical calculations that include both dissociation of the $c\bar{c}$ by a large gluon density and regeneration effects [16].

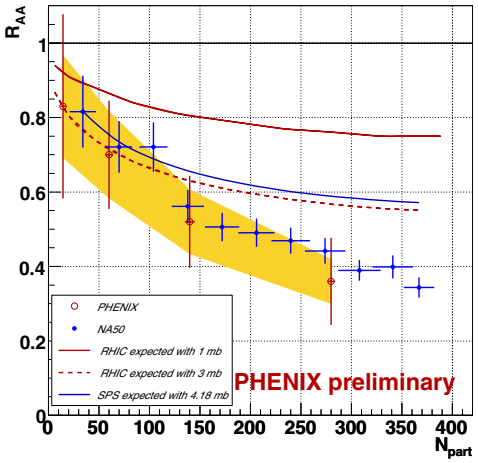

Fig. 14. (Colour on-line) 200 GeV RHIC J/ψ data [17] and 17.4 GeV NA50 [20] data plotted together *vs.* N_{part}, showing the universal dependence on number of participants. The curves are calculations for RHIC with shadowing and absorption cross-sections of 1 mb (red solid line) and 3 mb (red dashed line) [21]; and for NA50 with an absorption cross-section of 4.18 mb (blue solid line).

that through feed down normally provide about $\sim$ 40% of the J/ψ production. This picture provides a simple explanation for the nearly identical suppression observed at RHIC and the SPS seen in fig. 14. The J/ψ itself would be screened only for higher-energy collisions at the Large Hadron Collider (LHC).

8 Future - RHIC-II and detector upgrades

The luminosities obtained at RHIC are just beginning to reach levels where the more rare probes such as the Υ can be studied. In the future this will be improved further when RHIC-II, with its electron cooling, allows even higher luminosities. In addition upgrades of the RHIC detectors are underway, most notably adding high-resolution silicon vertex tracking in the inner regions of the large detectors (PHENIX and STAR) in order to make identification of heavy quarks more explicit via the separation of the primary and secondary vertices associated with the creation, propagation and subsequent decay of the heavy mesons. These detached vertex measurements of heavy quarks, along with the increasing luminosity will dramatically reduce systematic and statistical uncertainties in these measurements and will enable exclusive measurements of heavy quarks such as $B \to J/\psi X$.

9 Summary

In summary, evidence is mounting at RHIC for the creation of a new form of matter that is 1) dense and gives large energy losses and modifications of jet correlations for hadrons, 2) appears to be thermalized very early and to exhibit maximal flow as predicted by hydrodynamics models, with quark degrees of freedom, 3) also causes large energy loss and flow for heavy quarks, and 4) causes strong suppression, beyond that expected from cold–nuclear-matter effects, for the J/ψ. Future luminosity and detector upgrades will enable firming up and extending our understanding of these phenomena.

References

1. PHENIX Collaboration (S.S. Adler *et al.*), Phys. Rev. Lett. **94**, 232302 (2005).
2. M. Kaneta, N. Xu, nucl-th/0405068; P. Braun-Munzinger, K. Redlich, J. Stachel, nucl-th/0304013.
3. PHENIX Collaboration (S.S. Adler *et al.*), Phys. Rev. Lett. **91**, 072303 (2003).
4. STAR Collaboration (C. Adler *et al.*), Phys. Rev. Lett. **91**, 072304 (2003).
5. E. Shuryak, Nucl. Phys. A **783**, 31 (2007).
6. PHENIX Collaboration (S.S. Adler *et al.*), Phys. Rev. Lett. **96**, 202301 (2006).
7. I. Vitev, M. Gyulassy, Phys. Rev. lett. **89**, 252301 (2002); I. Vitev, J. Phys. G **30**, S791 (2004).
8. PHENIX Collaboration (S. Butsyk *et al.*), Nucl. Phys. A **774**, 669 (2006).
9. PHENIX Collaboration (X. Wang *et al.*), J. Phys. G **32**, S511 (2006).
10. H. van Hees, V. Greco, R. Rapp, Phys. Rev. C **73**, 034913 (2006); nucl-th/0608033.
11. K.J. Eskola, V.J. Kolhinen, R. Vogt, Nucl. Phys. A **696**, 729 (2001); L. Frankfurt, M. Strikman, Eur. Phys. J A **5**, 293 (1999).
12. L. McLerran, R. Venugopalan, Phys. Rev. D **49**, 2233; 3352 (1994).
13. T. Matsui, H. Satz, Phys. Lett. B **178**, 416 (1986).
14. F. Datta *et al.*, hep-lat/0409147.
15. S. Digal, S. Fortunato, H. Satz, Eur. Phys. J. C **32**, 547 (2004); hep-ph/0310354; A. Capella, E. Ferreiro, Eur. Phys. J. C **42**, 419 (2005); hep-ph/0505032.
16. L. Grandchamp, R. Rapp, G.E. Brown, Phys. Rev. Lett. **92**, 212301 (2004); hep-ph/0306077.

17. PHENIX Collaboration (H. Pereira da Costa *et al.*), Nucl. Phys. A **774**, 747 (2006).
18. PHENIX Collaboration (S.S. Adler *et al.*), Phys. Rev. Lett. **96**, 012304 (2006).
19. F. Karsch, D. Kharzeev, H. Satz, Phys. Rev. Lett. B **637**, 75 (2006); hep-ph/0512239.
20. NA50 Collaboration (B. Alessandro *et al.*), Eur. Phys. J. C **39**, 335 (2005).
21. R. Vogt, nucl-th/0507027 (2005) and private communication.